PERGAMON

Robotics and Computer-Integrated Manufacturing 14 (1998) 297–306

Robotics and Computer-Integrated Manufacturing

Using parallel line information for vision-based landmark location estimation and an application to automatic helicopter landing[1]

Zhi-Fang Yang, Wen-Hsiang Tsai*

Department of Computer and Information Science, National Chiao Tung University, Hsinchu, Taiwan 300, ROC

Received 17 June 1997; received in revised form 5 January 1998; accepted 23 February 1998

Abstract

An approach to landmark location estimation by computer vision techniques is proposed. The objective is to derive the position and the orientation of the landmark with respect to the vehicle by a single image. Such information is necessary for automatic vehicle navigation. This approach requires lower hardware cost and simple computation. The vanishing points of the parallel lines on the landmark are used to detect the landmark orientation. The detected vanishing points are used to derive the relative orientation between the landmark and the camera, which is then utilized to compute the landmark orientation with respect to the vehicle. The size of the landmark is used to determine the landmark position. Sets of collinear points are extracted from the landmark and their inter-point distances are computed. The positions of the collinear point sets are evaluated and used to determine the landmark position. Landing site location estimation by using the identification marking H on the helicopter landing site for automatic helicopter landing is presented as an application of the proposed approach. Simulations and experiments have been conducted to prove the feasibility of the proposed approach.

Keywords: Landmark; Vehicle navigation; Location estimation; Computer vision; Parallel lines; Vanishing points; Collinear points; Helicopter; Identification marking; Landing site; Automatic landing

1. Introduction

Autonomous vehicle navigation is a multi-disciplinary and demanding field. Among the research topics in this field, the location problem [1–8] is critical to any autonomous vehicle. To complete this task, the relative orientation and position between a vehicle and the environment should be obtained.

There are two kinds of vision-based approaches to solve this problem: the landmark approach [1–4] and the map approach [5–8]. The first kind of approach takes advantage of landmarks in the environment, for example, a door or a corner. Strategies for landmark detection are necessary. The knowledge of landmark locations is utilized to compute the desired location. The second kind of approach requires a detailed map of the environment. The features extracted from sensor data are matched with the features in the map to estimate the location parameters.

Landmark location estimation by computer vision techniques with the aim of lower hardware cost and simple computation is the main interest of this study. Emphasis is placed on the study of the automatic detection of the landmark orientation and position. Other issues like the extraction of the landmark from background and the problem of camera calibration are discussed elsewhere [9–11]. In landmark-based vehicle navigation, the relative position and the relative orientation between the vehicle and the landmark are the most critical information. An automatic landmark detection system should be able to find such information. An efficient detection method and a simple computation scheme are desired for real-time automatic detection.

Related works on landmark detection are surveyed as follows. Sato [1] used an image sequence of the circle of the heliport marking as the visual cue to estimate the position and the altitude of a helicopter with respect to the landing site. By utilizing the variations of the projections of the circle on the successive images taken by an on-board camera, a Kalman filter was designed to

*Corresponding author. Tel.: 886 03 5712121/ext. 56621; fax: 886 03 5721489; e-mail: whtsai@cis.nctu.edu.tw.

[1] This work was supported by National Science Council, Republic of China under Grant NSC-84-2213-E009-122.

0736-5845/98/$19.00
PII: S0736-5845(98)00007-6

recursively estimate the helicopter location. It is necessary to know if there is a circle, but the size of the circle need not be known. Chou and Tsai [2] used house corners as the standard mark. A monocular image of a house corner is first taken. The equations of the three lines going through the corner point were developed. Based on the knowledge of the distance from the camera to the ceiling, the relative location between the vehicle and the corner can be uniquely determined. Atiya and Hager [3] used the vertical edges in the environment as the visual landmarks. A stored map was also utilized to compute the robot location by using those correspondences. The advantages include the possibility to describe the observation error by a single geometric tolerance, the ability to recognize correspondences, and fast computation. Gilg and Schmidt [4] developed an approach to landmark-based vehicle guidance in corridors. A video sensor system is used for landmark detection. A symbolic course description is used to specify motion tasks.

In this study, a single image acquired by a camera mounted on the vehicle is used to achieve the estimation of the landmark position and orientation relative to the vehicle. The vanishing points of the parallel lines extracted from the landmark are detected to derive the orientation of the landmark relative to the vehicle. The size of the landmark is used to compute the landmark position. The proposed approach has several advantages. First, the annoying image correspondence problem is not involved since only a single image is needed to complete the estimation process. Lower hardware cost is required because only one camera is used to acquire passive data. Finally, the computation of the parameters is based on the use of analytic formulas and this increases the computation speed and the possibility of hardware implementation of this method.

A case study of landing site location estimation by using a special landmark, the identification marking H defined by the International Civil Aviation Organization (ICAO) [12], on the helicopter landing site is presented. Automatic helicopter landing is highly desired since landing maneuver is one of the most difficult skills demanded of the helicopter pilot. A large percentage of accidents were attributed to the landing phase of a flight. Added to the fact is that helicopters are more and more popular tools for transportation due to their high mobility and low cost. The proposed approach shows the possibility of automatic detection of the landing site location by computer vision techniques.

In the remainder of this paper, Section 2 includes some definitions used in this study. In Section 3, the derivation of the landmark orientation by the use of the parallel lines extracted from the landmark is described. Section 4 includes the derivation of the landmark position by the use of the size of the landmark. The case study of landing site location estimation by using the proposed approach is described in Section 5. Finally, some conclusions are given in Section 6.

2. Problem definition

In this study, it is desired to compute the landmark position with respect to the vehicle, denoted as $(x_m, y_m, z_m)^T$, and the landmark orientation, denoted as α_m, β_m, and γ_m, which represent the angles between the three vehicle body axes and the three main axes of the coordinate system describing the landmark geometry from the viewpoint of the vehicle. In the following, the definitions and notations used in this study are introduced.

Two sets of orthogonal parallel lines are supposed to exist on the landmark. For convenience, the two sets of parallel lines are denoted as line set A and line set B, and each line in line set A is perpendicular to each in B. More specifically, as shown in Fig. 1, the two sets are $A = \{A_1, A_2, \ldots, A_{p-1}, A_p\}$ and $B = \{B_1, B_2, \ldots, B_{q-1}, B_q\}$. Each intersection of these two sets of lines is denoted as p_{ij} to indicate that it is the intersection of lines A_i and B_j. Also, we define H_i to include all the collinear intersections of $p_{i1}, p_{i2}, \ldots, p_{i(q-1)}$, and p_{iq} on line A_i, and define V_j to include all the collinear intersections of $p_{1j}, p_{2j}, \ldots, p_{(p-1)j}$, and p_{pj} on line B_j. For example, $H_1 = \{p_{11}, p_{12}, \ldots, p_{1(q-1)}, p_{1q}\}$ and $V_2 = \{p_{12}, p_{22}, \ldots, p_{(p-1)2}, p_{p2}\}$. Thus, all intersections can be grouped into $(p + q)$ sets of collinear points with p or q points in each set. The landmark position is defined as the center point of the square region $p_{11}\ p_{1q}\ p_{pq}\ p_{p1}$. This position is chosen to represent the location of the landmark in this study.

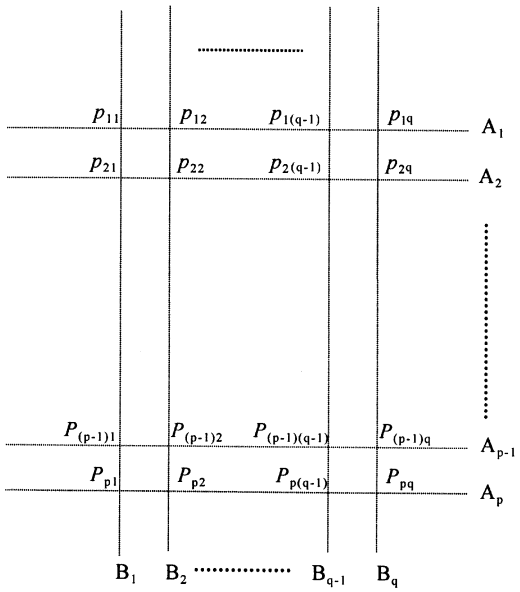

Fig. 1. Illustration of the landmark and the notations used in this study.

Several coordinate systems used in this study are shown in Fig. 2. The camera mounted on the vehicle has a camera coordinate system (CCS), denoted as x–y–z. The corresponding image plane (ICS) is denoted as u–v. The three axes of the vehicle body form a vehicle coordinate system (VCS), whose names are: the normal axis, the lateral axis, and the longitudinal axis. It is assumed reasonably that the line directions of these three-body axes in the CCS are pre-known, denoted as $\mathbf{d}_{\text{normal}}$, $\mathbf{d}_{\text{lateral}}$, and $\mathbf{d}_{\text{long}}$. To describe the relative orientation between the landmark and the vehicle, we need another coordinate system, called the global coordinate system (GCS), which is denoted as x'–y'–z'. The y'-axis and the z'-axis are set on the ground and parallel to the line sets A and B with the origin located at the center point of the landmark. The landmark position is defined as $(x_m, y_m, z_m)^T$ which is the center point of the landmark in the VCS. The landmark orientation is defined as α_m, β_m, and γ_m, which are the angles between the axes of the VCS and the GCS with respect to the vehicle, respectively.

The point transformation between the CCS and the VCS is needed to transform the computed landmark position in the CCS into the VCS. This transformation [17] can be written as

$$(x', y', z') = (x - x_d, y - y_d, z - z_d) \times \begin{bmatrix} r_{11} & r_{12} & r_{13} \\ r_{21} & r_{22} & r_{23} \\ r_{31} & r_{32} & r_{33} \end{bmatrix}, \quad (1)$$

where $r_{11} = \cos\theta\cos\psi + \sin\theta\sin\phi\sin\psi$, $r_{12} = -\sin\theta\cos\phi$, $r_{13} = \sin\theta\sin\phi\cos\psi - \cos\theta\sin\psi$, $r_{21} = -\cos\theta\sin\phi\sin\psi + \sin\theta\cos\psi$, $r_{22} = \cos\theta\cos\phi$, $r_{23} = -\cos\theta\sin\phi\cos\psi - \sin\theta\sin\psi$, $r_{31} = \cos\phi\sin\psi$, $r_{32} = \sin\phi$, $r_{33} = \cos\phi\cos\psi$, and θ, ϕ, and ψ are the pan, tilt, and swing angles of the vehicle, respectively, with respect to the CCS; (x_d, y_d, z_d) is the translation vector from the origin of the CCS to the origin of the VCS. The three orientation angles and the translation vector are all known in advance by a calibration process [13].

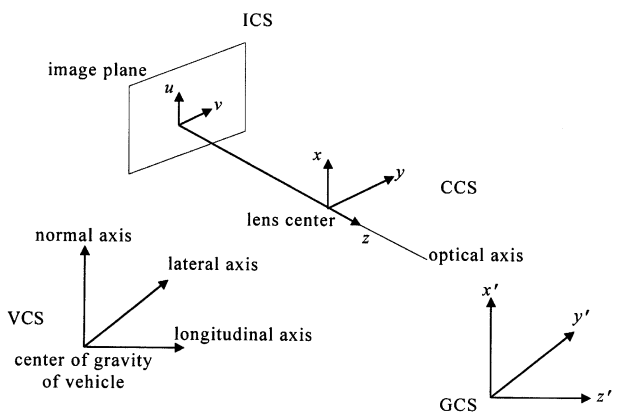

Fig. 2. The camera coordinate system x–y–z, the image coordinate system u–v, the global coordinate system x'–y'–z', and the vehicle coordinate system.

3. Computing landmark orientation from parallel lines on landmark

In this study, the vanishing points of the line sets A and B of the parallel lines extracted from the landmark are used to derive the landmark orientation. The vanishing points contain the information of the 3D line directions of these two sets of parallel lines in the CCS. These line directions are used to compute the orientation of the landmark with respect to the vehicle.

In the following, we first describe the relationship between a vanishing point and its corresponding 3D parallel lines. Next, the detection of the desired vanishing points and the derivation of the landmark orientation are described.

3.1. Vanishing point of a set of parallel lines

As is well known, the image lines of a set of 3D parallel lines intersect at a vanishing point on the image plane. This important property indicates that the 3D line direction of the set of parallel lines can be derived from their vanishing point. In this study, this property is utilized to get the orientation of the landmark.

Consider a 3D line L represented by a set of points

$$L = \{(x, y, z)^T \mid (x, y, z)^T = (p_1, p_2, p_3)^T + \lambda(d_1, d_2, d_3)^T \text{ for some real value } \lambda\}. \quad (2)$$

The line L passes through the point $(p_1, p_2, p_3)^T$ and has the line direction $(d_1, d_2, d_3)^T$. The image point $(u, v)^T$ of 3D point $(x, y, z)^T$ on line L can be written as

$$(u, v)^T = \left(f\frac{x}{z}, f\frac{y}{z}\right)^T = \left(f\frac{p_1 + \lambda d_1}{p_3 + \lambda d_3}, f\frac{p_2 + \lambda d_2}{p_3 + \lambda d_3}\right)^T, \quad (3)$$

where f is the focal length of the camera. A vanishing point $(u_\infty, v_\infty)^T$ can be expected if $\lambda \to \infty$ and $d_3 \neq 0$; that is,

$$(u_\infty, v_\infty)^T = \left(f\frac{d_1}{d_3}, f\frac{d_2}{d_3}\right)^T. \quad (4)$$

As can be seen, the location of the vanishing point only depends on the direction of the line and the focal length. The above derivation indicates an important fact: if a vanishing point $(u_\infty, v_\infty)^T$ is detected on the image

plane, the direction of line L can be uniquely determined from Eq. (4) to be

$$(d_1, d_2, d_3)^{\mathrm{T}} = \frac{1}{\sqrt{u_\infty^2 + v_\infty^2 + f^2}} (u_\infty, v_\infty, f)^{\mathrm{T}}, \tag{5}$$

where unit length is superimposed on the line direction $(d_1, d_2, d_3)^{\mathrm{T}}$. Other findings about vanishing points can be found in [14].

3.2. Derivation of landmark orientation by vanishing point detection

Now, we discuss how to compute the three angles, α_{m}, β_{m}, and γ_{m}, between the axes of the VCS and the GCS, which describe the landmark orientation relative to the vehicle. These angles are computed in the CCS. First, the line directions of the three axes of the GCS in the CCS should be computed. The line directions of the y'-axis and the z'-axis of the GCS in the CCS can be computed from their corresponding vanishing points in the ICS. After these two line directions are computed, obviously, the line direction of the x'-axis of the GCS in the CCS can be obtained by their cross product. Recall that the line directions of the three axes of the VCS in the CCS are known in advance. Now that the line directions of the axes of the VCS and the GCS in the CCS are all known, the landmark orientation, in terms of the desired angles, α_{m}, β_{m}, and γ_{m}, can be obtained by inner product. The details of the derivations are described next.

First, the computation of the line directions of the x'-, y'- and z'-axis of the GCS in the CCS by the use of vanishing points is as follows. The vanishing point of the image lines produced by line set A and that by line set B are used to derive the line directions of the y'-axis and the z'-axis. At first, the intersections of every two lines in line set A are computed. Totally, $(p^2 - p)/2$ intersections can be obtained because there are p lines in line set A. Each intersection is treated as a candidate vanishing point. The coordinates of all candidate vanishing points are averaged to obtain the coordinates of a representative point, which is then taken to be the vanishing point of line set A. Then, the line direction derived by Eq. (5) is used as the desired line direction of line set A in the CCS, which in turn is taken to be the line direction of the y'-axis in the CCS, and is denoted as $\mathbf{d}_{y'}$. The same process is followed for line set B, and the result is denoted as $\mathbf{d}_{z'}$. Finally, $\mathbf{d}_{x'}$, the line direction of the x'-axis in the CCS, is computed as the cross product, $\mathbf{d}_{y'} \times \mathbf{d}_{z'}$. The derived formulas are as follows:

$$\mathbf{d}_{x'} = \mathbf{d}_{y'} \times \mathbf{d}_{z'}, \tag{6}$$

$$\mathbf{d}_{y'} = \frac{1}{\sqrt{U_a^2 + V_a^2 + f^2}} (U_a, V_a, f)^{\mathrm{T}}, \tag{7}$$

$$\mathbf{d}_{z'} = \frac{1}{\sqrt{U_b^2 + V_b^2 + f^2}} (U_b, V_b, f)^{\mathrm{T}}, \tag{8}$$

where (U_a, V_a) and (U_b, V_b) are the averaged coordinates of the intersections of the lines in line sets A and B in the ICS, respectively.

Then, the landmark orientation, α_{m}, β_{m}, and γ_{m}, can be computed from the inner products of $\mathbf{d}_{x'}$ and $\mathbf{d}_{\mathrm{normal}}$, $\mathbf{d}_{y'}$ and $\mathbf{d}_{\mathrm{lateral}}$, and $\mathbf{d}_{z'}$ and $\mathbf{d}_{\mathrm{long}}$, respectively, to get the following result:

$$\cos(\alpha_{\mathrm{m}}) = (\mathbf{d}_{x'} \cdot \mathbf{d}_{\mathrm{normal}})/(\|\mathbf{d}_{x'}\| \, \|\mathbf{d}_{\mathrm{normal}}\|), \tag{9}$$

$$\cos(\beta_{\mathrm{m}}) = (\mathbf{d}_{y'} \cdot \mathbf{d}_{\mathrm{lateral}})/(\|\mathbf{d}_{y'}\| \, \|\mathbf{d}_{\mathrm{laeral}}\|), \tag{10}$$

$$\cos(\gamma_{\mathrm{m}}) = (\mathbf{d}_{z'} \cdot \mathbf{d}_{\mathrm{long}})/(\|\mathbf{d}_{z'}\| \, \|\mathbf{d}_{\mathrm{long}}\|). \tag{11}$$

4. Computing landmark position from size of landmark

The size of the landmark is used to derive the landmark position in this study. As can be seen $(p + q)$ sets of collinear points, H_i's and V_j's, can be detected on the landmark. The inter-point distances of each collinear point set are known in advance. With the inter-point distances, the 3D locations of all collinear points can be computed and used to determine the landmark position.

In the following, we first describe the derivation of 3D point locations of a set of collinear points with known inter-point distances. Next, the derived formulas are used to compute the landmark position.

4.1. Computing 3D locations of collinear points with known inter-point distances

Let the first point of the N collinear points be $\mathbf{p} = (p_1, p_2, p_3)^{\mathrm{T}}$ and the line direction be $\mathbf{d} = (d_1, d_2, d_3)^{\mathrm{T}}$. The N collinear points can be described as: $\mathbf{p}$, $\mathbf{p} + \delta_1\mathbf{d}$, $\mathbf{p} + \delta_2\mathbf{d}$, $\mathbf{p} + \delta_3\mathbf{d}$, …, and $\mathbf{p} + \delta_{N-1}\mathbf{d}$ where δ_n is the distance between the first and the $(n + 1)$st collinear points. According to the perspective transformation principle, the image point $(u_n, v_n)^{\mathrm{T}}$ of the $(n + 1)$st point $\mathbf{p} + \delta_n\mathbf{d}$ on the image plane can be written as follows:

$$(u_n, v_n)^{\mathrm{T}} = \left(f\frac{p_1 + \delta_n d_1}{p_3 + \delta_n d_3}, f\frac{p_2 + \delta_n d_2}{p_3 + \delta_n d_3} \right)^{\mathrm{T}}, \tag{12}$$

where $n = 0, 1, \ldots, N - 1$. The linear system below is the result of transforming Eq. (12) into matrix form for $n = 0, 1, \ldots, N - 1$:

$$\mathbf{A}\mathbf{p} = \mathbf{b}, \tag{13}$$

where

$$\mathbf{A} = \begin{pmatrix} f \ldots f & 0 \ldots 0 \\ 0 \ldots 0 & f \ldots f \\ -u_0 \ldots -u_{N-1} & -v_0 \ldots -v_{N-1} \end{pmatrix}^{\mathrm{T}},$$

$$\mathbf{p} = (p_1, p_2, p_3)^{\mathrm{T}}.$$

and

$$\mathbf{b} = (\delta_0(u_0 d_3 - f d_1), \ldots, \delta_{N-1}(u_{N-1} d_3 - f d_1), \delta_0(u_0 d_3 - f d_2), \ldots, \delta_{N-1}(u_{N-1} d_3 - f d_2))^{\mathrm{T}},$$

where $\mathbf{p} = (p_1, p_2, p_3)^{\mathrm{T}}$ is the unknowns. In this study, QR-decomposition [15] is used to solve this linear system, which is treated as a least-squares problem. The details are described as follows.

First, the Gram-Schmidt process [15] is used to get the unnormalized QR-decomposition of $\mathbf{A}$ denoted as $\mathbf{A} = \mathbf{Q}_0\mathbf{R}_0$. By normalizing $\mathbf{Q}_0$, we can write $\mathbf{A}$ in its normalized QR-decomposition form denoted as $\mathbf{A} = \mathbf{QR}$. The result is as follows:

$$\mathbf{A} = \mathbf{QR}, \tag{14}$$

where

$$\mathbf{Q} = \begin{pmatrix} \frac{1}{\sqrt{N}} & \cdots & \frac{1}{\sqrt{N}} & 0 & \cdots & 0 \\ 0 & \cdots & 0 & \frac{1}{\sqrt{N}} & \cdots & \frac{1}{\sqrt{N}} \\ \frac{U-u_0}{q} & \cdots & \frac{U-u_{N-1}}{q} & \frac{V-v_0}{q} & \cdots & \frac{V-v_{N-1}}{q} \end{pmatrix}^{\mathrm{T}}$$

and

$$\mathbf{R} = \begin{pmatrix} \sqrt{N}f & 0 & 0 \\ 0 & \sqrt{N}f & 0 \\ \frac{U}{\sqrt{N}} & \frac{V}{\sqrt{N}} & q \end{pmatrix}$$

with

$$q = \sqrt{S_U + S_V - \frac{U^2}{N} - \frac{V^2}{N}},$$

$$U = \sum_{i=0}^{N-1} u_i, \qquad V = \sum_{i=0}^{N-1} v_i,$$

$$S_U = \sum_{i=0}^{N-1} u_i^2, \quad \text{and} \quad S_V = \sum_{i=0}^{N-1} v_i^2.$$

Solving this system by the criterion of minimum least squares is equivalent to finding $\mathbf{p}$ in the following system:

$$\mathbf{RP} = \mathbf{Q}^{\mathrm{T}}\mathbf{b}, \tag{15}$$

where $\mathbf{Q}^{\mathrm{T}}\mathbf{b}$ can be derived to be

$$\mathbf{Q}^{\mathrm{T}}\mathbf{b} = \left(\frac{1}{N}\sum_{i=0}^{N-1}\delta_i(u_i d_3 - f d_1), \frac{1}{N}\sum_{i=0}^{N-1}\delta_i(v_i d_3 - f d_2), \frac{1}{q}\sum_{i=0}^{N-1}\left(\delta_i(u_i d_3 - f d_1)\left(-u_i + \frac{U}{N}\right) + \delta_i(v_i d_3 - f d_2)\left(-v_i + \frac{V}{N}\right)\right)\right)^{\mathrm{T}} = (q_1, q_2, q_3)^{\mathrm{T}}. \tag{16}$$

With $(q_1, q_2, q_3)^{\mathrm{T}}$, $\mathbf{p}$ can be solved immediately by simple back-substitution to get the desired result as discussed next.

Remember that there are two line directions for each line; one is exactly the opposite of the other. But in Eq. (5), a specific one is selected. This selection may be the opposite one for the previously decided inter-point distances δ_i. For this reason, we have to check the answer computed so far. If the answer indicates that the computed point $(p_1, p_2, p_3)^{\mathrm{T}}$ is behind the camera, we know that the opposite line direction is chosen. To get the correct answer, the only action needed is to negate the computed $(p_1, p_2, p_3)^{\mathrm{T}}$. The final result is as follows:

if $q_3 > 0$, then

$$(p_1, p_2, p_3)^{\mathrm{T}} = \left(\frac{1}{\sqrt{N}f}q_1 + \frac{U}{Nfq}q_3, \frac{1}{\sqrt{N}f}q_2 + \frac{V}{Nfq}q_3, \frac{1}{q}q_3\right)^{\mathrm{T}},$$

otherwise,

$$(p_1, p_2, p_3)^{\mathrm{T}} = -1 \times \left(\frac{1}{\sqrt{N}f}q_1 + \frac{U}{Nfq}q_3, \frac{1}{\sqrt{N}f}q_2 + \frac{V}{Nfq}q_3, \frac{1}{q}q_3\right)^{\mathrm{T}}. \tag{17}$$

4.2. Computing landmark position from sets of collinear points

The point locations of the sets of collinear points, H_i's and V_j's, are derived as follows. For each collinear point set, suppose that the corresponding line direction in the CCS is $\mathbf{d} = (d_1, d_2, d_3)^{\mathrm{T}}$. Assume $\mathbf{d} = \mathbf{d}_{y'}$ for sets H_i's and $\mathbf{d} = \mathbf{d}_{z'}$ for sets V_j's. Actually, the collinear points can be expressed as $\mathbf{p}$, $\mathbf{p} + \delta_1\mathbf{d}$, …, $\mathbf{p} + \delta_{p-2}\mathbf{d}$, and $\mathbf{p} + \delta_{N-1}\mathbf{d}$, where $N = q$ for sets H_i's, $N = p$ for sets V_j's, and $\delta_1, \ldots, \delta_{N-1}$ are the inter-point distances for that collinear point set. Now, the location of $\mathbf{p}$ can be computed directly by Eq. (17). Then, the locations of all $p + q$ collinear point sets can also be computed.

According to our experimental experience, we choose the computed locations of the innermost points of the landmark to evaluate the landmark position. The averaged coordinates of these points are computed to obtain a candidate landmark position. Two candidates positions can be obtained since both sets H_i's and V_j's are used. Their averaged coordinates are computed to be the final landmark position in the CCS. Finally, this position

is transformed by Eq. (1) into $(x_m, y_m, z_m)^T$ in the VCS, as the desired landmark position.

5. Case study: Landing site location estimation by identification marking for automatic helicopter landing

In this section, a case study of the application of the proposed approach is presented. A single image of the landmark, the identification marking H, on the helicopter landing site acquired by a camera mounted on the helicopter is used to achieve the estimation of the landing site location. The vanishing points of parallel lines extracted from the shape of the identification marking H on the landing site are detected to derive the orientation of the landing site relative to the helicopter. The international standard size of the identification marking H defined by the ICAO [12] is used to compute the landing site position.

The standard identification marking H on the landing site defined by the ICAO is shown in Fig. 3. According to the standards adopted by ICAO [12], an identification marking should be provided on the landing site. The identification marking consists mainly of a letter H, white in color. The dimensions of the marking should not be smaller than those shown in Fig. 3. Also, the marking should be oriented in such a way that the cross arm of the H is at right angle to the preferred final approach direction of the helicopter. As discussed in Section 2, the two sets of parallel lines in the figure may be taken as $A = \{A_1, A_2, A_3, A_4\}$ and $B = \{B_1, B_2, B_3, B_4\}$. Each line in line set A has the same direction as that of the cross arm of the H. H_i includes all the collinear vertices of p_{i1}, p_{i2}, p_{i3}, and p_{i4} on line A_i, and V_j includes all the collinear vertices of p_{1j}, p_{2j}, p_{3j}, and p_{4j} on line B_j. Thus, all vertices of the H can be grouped into eight sets of collinear points with four points in each set. The position of the marking is defined as the center point of the cross arm of the H. This position is chosen to represent the location of the landing site.

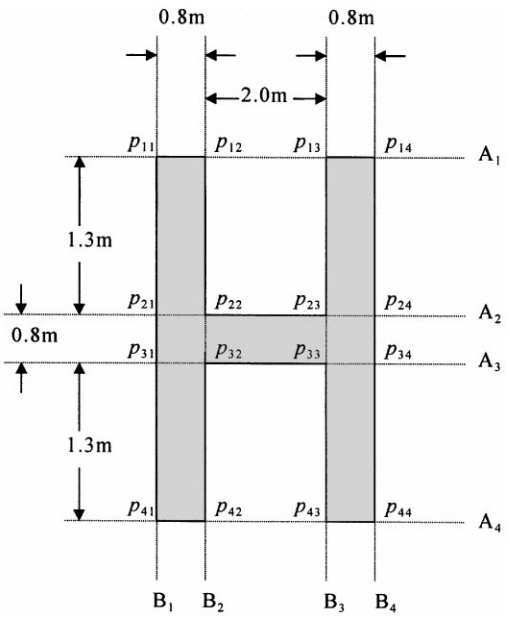

Fig. 3. Illustration of the identification marking H and the notations used in this study.

5.1. Landing site location by identification marking

After line set A and line set B are extracted from the acquired image of the identification marking. The process described in Section 3.2 is followed for the estimation of the landing site orientation. At first, the intersections of every two lines in line set A are computed. Totally, six intersections can be obtained because there are four lines in line set A. Each intersection is treated as a candidate vanishing point. The coordinates of all six candidate vanishing points are averaged to be the vanishing point of line set A. The same process is followed for line set B. By Eq. (6)–(8), the desired axis directions of the GCS in the CCS, $\mathbf{d}_{x'}$, $\mathbf{d}_{y'}$, and $\mathbf{d}_{z'}$, are obtained, respectively. Then, the landing site orientation, α_m, β_m, and γ_m can be computed by Eqs. (9)–(11).

The size of the identification marking H is used to derive the landing site position. Eight sets of collinear points, H_i's and V_j's, can be detected on the identification marking. For each collinear point set, suppose that the corresponding line direction in the CCS is $\mathbf{d} = (d_1, d_2, d_3)^T$. Take $\mathbf{d} = \mathbf{d}_{y'}$ for sets H_i's and $\mathbf{d} = \mathbf{d}_{z'}$ for sets V_j's. The collinear points can be expressed as $\mathbf{p}$, $\mathbf{p} + \delta_1\mathbf{d}$, $\mathbf{p} + \delta_2\mathbf{d}$, and $\mathbf{p} + \delta_3\mathbf{d}$, where δ_1, δ_2, and δ_3 are the inter-point distances. We have $N = 4$ in this case. In the ICS, suppose that the corresponding image points are detected at $(u_0, v_0)^T$, $(u_1, v_1)^T$, $(u_2, v_2)^T$, and $(u_3, v_3)^T$. The location of $\mathbf{p}$ can be computed by Eq. (17) to be as follows:

if $q_3 > 0$

$$(p_1, p_2, p_3)^T = \left(\frac{1}{2f}q_1 + \frac{U}{4fq}q_3, \frac{1}{2f}q_2 + \frac{V}{4fq}q_3, \frac{1}{q}q_3\right)^T,$$

otherwise,

$$(p_1, p_2, p_3)^T = -1 \times \left(\frac{1}{2f}q_1 + \frac{U}{4fq}q_3, \frac{1}{2f}q_2 + \frac{V}{4fq}q_3, \frac{1}{q}q_3\right)^T, \quad (18)$$

where

$$U = u_0 + u_1 + u_2 + u_3,$$
$$V = v_0 + v_1 + v_2 + v_3,$$
$$S_U = u_0^2 + u_1^2 + u_2^2 + u_3^2,$$
$$S_V = v_0^2 + v_1^2 + v_2^2 + v_3^2,$$

$$q = \sqrt{S_U + S_V - (U^2/4) - (V^2/4)},$$

$$q_1 = \frac{1}{2}\sum_{i=0}^{3} \delta_i(u_i d_3 - f d_1),$$

$$q_2 = \frac{1}{2}\sum_{i=0}^{3} \delta_i(v_i d_3 - f d_2),$$

$$q_3 = \frac{1}{q}\sum_{i=0}^{3} \left(\delta_i(u_i d_3 - f d_1)\left(-u_i + \frac{U}{4}\right) + \delta_i(v_i d_3 - f d_2)\left(-v_i + \frac{V}{4}\right)\right).$$

And the other three collinear points can be computed according to the inter-point distances easily. Thus, the locations of the eight collinear point sets can be computed.

As described in Section 4.2, the computed locations of the four inner vertices of the marking, p_{22}, p_{23}, p_{32}, and p_{33}, are chosen to evaluate the landing site position. The averaged coordinates of these four points are computed to be the candidate landing site position. Two candidates can be obtained since both sets H_i's and V_j's are used. Their averaged coordinates are then computed to be the landing site position in the CCS. Finally, this position is transformed by Eq. (1) into $(x_m, y_m, z_m)^T$ in the VCS, as the desired landing site position.

5.2. Image processing techniques

In this study, sets of parallel lines and sets of collinear points are extracted from the identification marking H by image processing techniques. The employed methods are described as follows.

For each acquired landing site image, line sets A and B are extracted first by images-processing techniques, including thresholding, edge detection, and line detection. The identification marking contrasts well with the background since it is originally a visual aid for the pilot. It is reasonable to pre-select a threshold value to segment the identification marking H in the image. An edge detector proposed by Person and Robinson [16] is employed to find the edge points of the marking. This computational edge detector yields clean edge points rather than thick bands or clouds of edge points found by other edge detectors [17]. The Hough transform [17] is applied to the resulting edge points to detect candidate lines. The detected candidate lines are then merged into a smaller number of lines if they have similar line slopes and the center points of the corresponding line segments on the acquired image are close enough. The merged lines are further improved by least-square-error line fitting. As we can expect, eight lines are detected and can be easily divided into two sets of lines. Eight sets of collinear points are then computed by finding the intersections of each line with the four lines in the other line set. In the following, the identification of line sets A and B from these two sets of lines is described.

The cross ratio [14] is adopted as a feature to recognize line sets A and B from the two detected line sets. The dimension of the identification marking is fixed. This indicates that the cross ratio of the set of collinear points H_i's or V_j's is known in advance. By definition, the cross ratio of H_i's is 0.082 and the cross ratio of V_j's is 0.585. As we can see, these two values are so different that the cross ratio is indeed an effective feature. Now, for these two sets of detected lines, all sets of collinear points are computed and their cross ratios are evaluated. The averaged cross ratio of each line set is calculated. Thus, line sets A and B can be recognized from these two detected line sets by simple comparison of the averaged cross ratios and the pre-known cross ratios.

After line sets A and B are found, the detection of the desired elements for the proposed approach is finished. An example of image processing results is shown in Fig. 4.

5.3. Experimental results

Simulations have been done to verify the correctness of the formulas derived in this section with noise-free data. The computation results are accurate. The details are as follows. A global coordinate system is created as the GCS and the identification marking is constructed in the GCS as defined in Section 2. The position and orientation of the camera are randomly selected in the GCS. In the simulation, we suppose that the CCS and the VCS are identical. Thus, the landing site orientation is the relative orientation between the CCS and the GCS. And the landing site position is the location of the center of the identification marking in the CCS. The equations of the lines forming the identification marking in the GCS are transformed into the ICS. The derived formulas are used to compute the landing site orientation and position, which are then compared with the correct data. The relative errors of the landing site orientation and position are both zero for each test data set.

Experiments on real images and error analysis have also been conducted. In this study, it is assumed that the

Table 1
Experimental results for landing site orientation

	Computed landing site orientation $(\alpha_h, \beta_h, \gamma_h)$ (°)	Angle between dy′ and dz′ (°)	Relative error (°)
1	(44.7933, 152.0871, 50.6771)	88.0102	1.9898
2	(48.8344, 134.9871, 57.6695)	86.6913	3.3087
3	(132.3595, 34.3329, 52.6991)	88.0831	1.9169
4	(127.6449, 54.7279, 57.5232)	84.3886	5.6114
5	(44.9055, 123.8360, 63.2140)	84.7896	5.2104

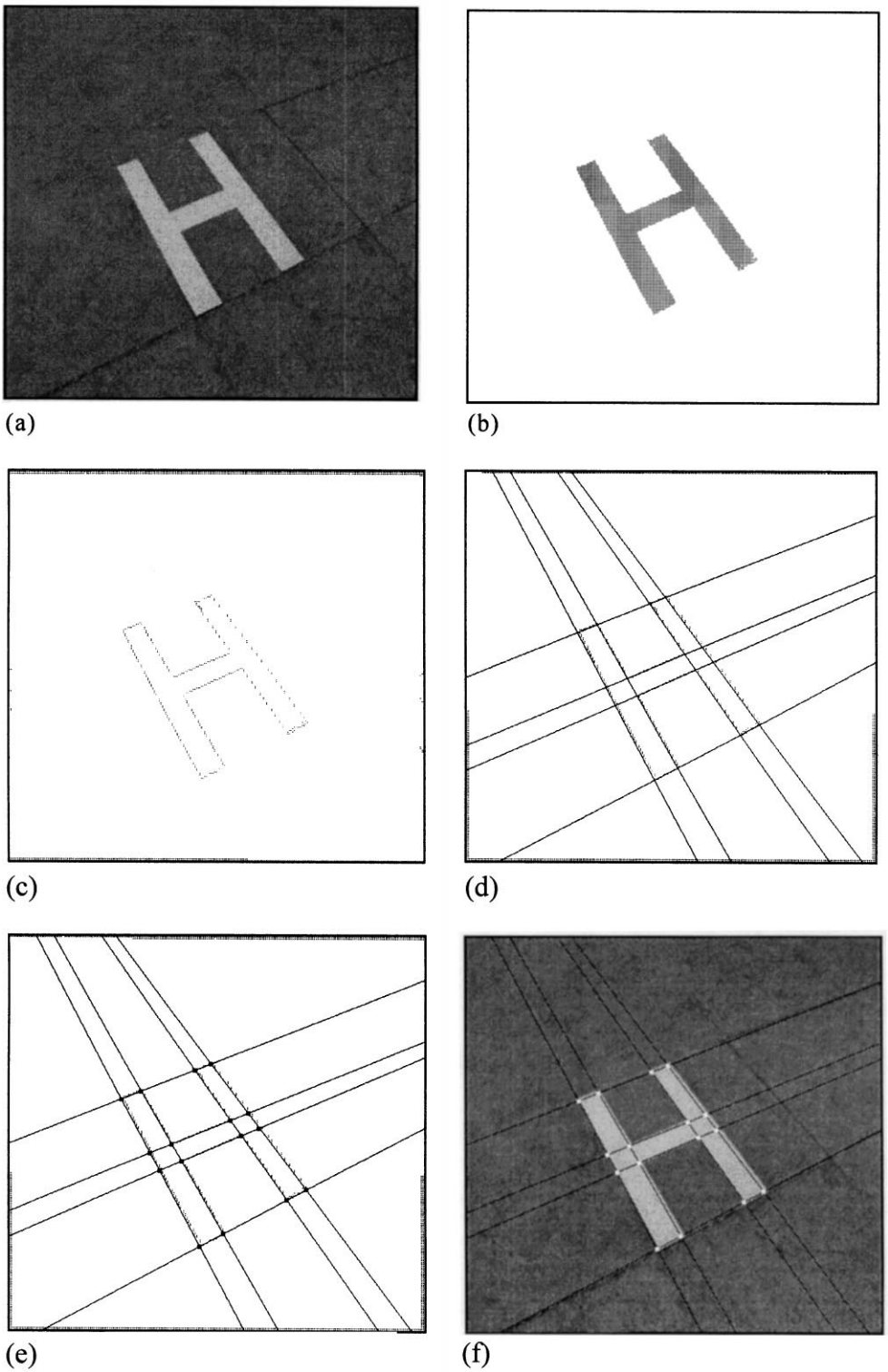

Fig. 4(a)–(f). An image processing result. (a) The original image. (b) The result of thresholding. (c) The result of edge detection. (d) The result of line detection. (e) The result of collinear points detection. (f) The image processing result shown on the original image.

identification marking has been extracted from the image of the landing site and zoomed into a certain size as the initial input to the proposed method. An identification marking satisfying the requirements of the ICAO was made. The proportion of the length is 10 : 1. For convenience, the CCS and the VCS are supposed to be identical. Images of the marking were taken at different positions and directions, and processed to get the landing site

orientation and position. The computed results are not compared with manual measurements to avoid manual error. Instead, two kinds of measurements are used to compute the error. One is the relative error of the angle between the computed landing site orientations, $\mathbf{d}_{y'}$ and $\mathbf{d}_{z'}$ in the CCS, compared with 90° which is the correct angle if noise-free data are available. The result is shown in Table 1. The average error is about 3.6°. The other is the relative error of the projection of the computed landing site position on the image (Fig. 5), the center of the

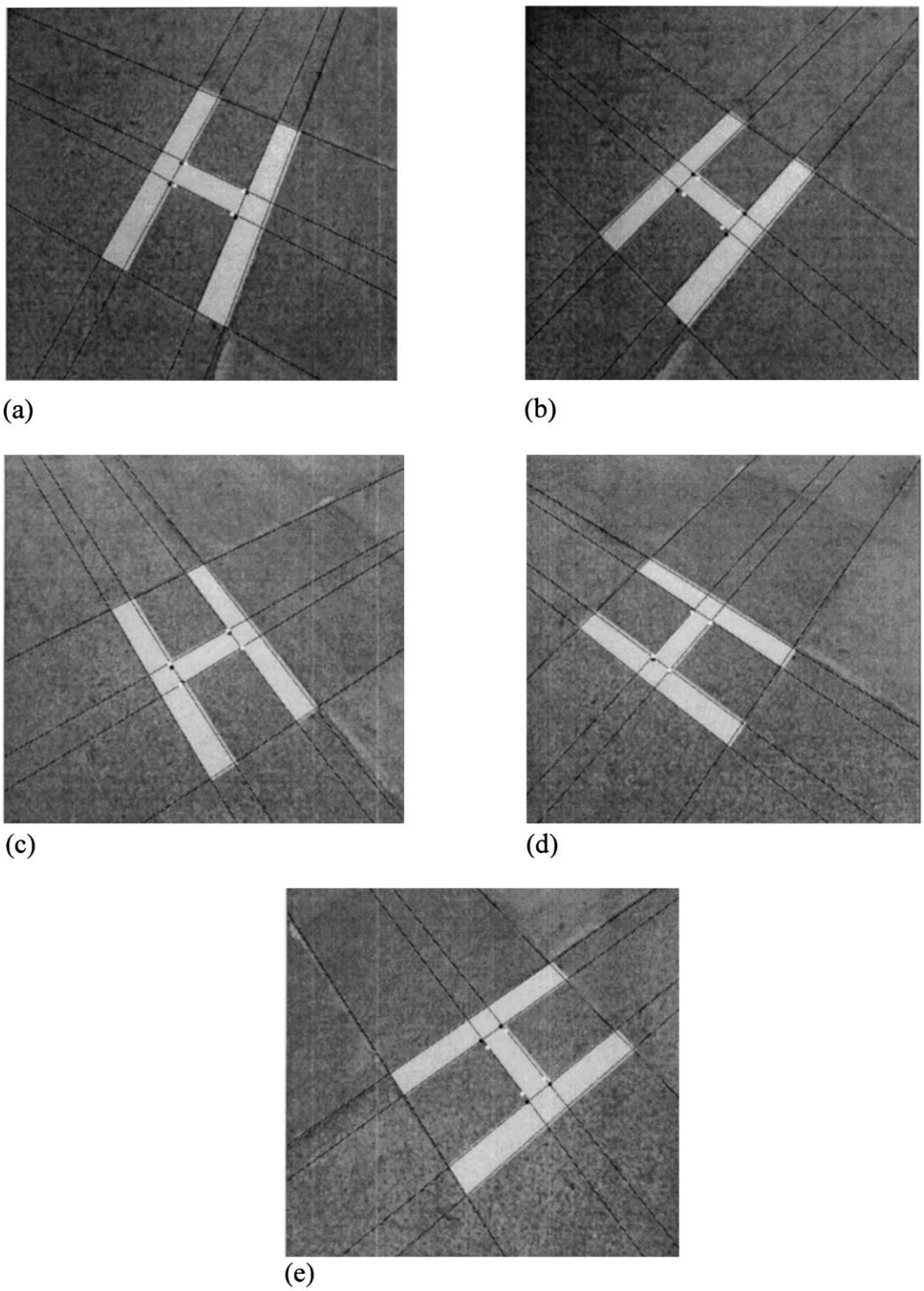

Fig. 5(a)–(e). Projections of the computed four inner vertices of the marking used to evaluate the landing site position on the original images. The white points show the results computed by the collinear points H_i's and $\mathbf{d}_{y'}$, and the back ones by V_i's and $\mathbf{d}_{z'}$.

Table 2
Experimental results for landing site position

	Computed landing site position (x, y, z)	Projection of computed landing site position (u, v)	Landing site position on acquired image (u, v)	Relative error (pixel, pixel)
1	(44.7933, 152.0871, 50.6771)	(263.59, 248.07)	(263.27, 249.27)	(0.32, 1.20)
2	(48.8344, 134.9871, 57.6695)	(240.48, 230.65)	(240.94, 231.11)	(0.54, 0.46)
3	(132.3595, 34.3329, 52.6991)	(257.86, 220.51)	(259.57, 222.93)	(2.71, 2.42)
4	(127.6449, 54.7279, 57.5232)	(202.97, 245.76)	(203.99, 246.89)	(1.02, 1.13)
5	(44.9055, 123.8360, 63.2140)	(294.03, 257.86)	(295.18, 257.37)	(1.15, 0.49)

marking, compared with the extracted landing site position in the acquired image. The result is shown in Table 2. The average error is about 1.144 pixel. Both measurements show acceptable results.

For each acquired image, the image processing time is about 0.66 s and the computation time of the analytic formulas is less than 0.001 s. The estimation is based on a personal computer with a CPU of Pentium 166 MHz. By improving the software efficiency and the hardware equipment, even faster speeds can be attained. The requirement of the little computation time for the derived formulas is due to their analytic forms. It is an advantage of the proposed approach, compared to the recursive methods used by some other approaches. For example, in Escalera et al. [5], the step of the extended Kalmen filter takes a time of about 0.1 s.

6. Conclusions

In this study, an approach to estimate the landmark location by computer vision techniques using parallel line information on the landmark is proposed. This approach uses single images to avoid motion analysis which is complicated and time consuming. By taking the advantage of the fixed size and the parallel lines of the landmark, only computation of some analytic formulas are needed, which speeds up the estimation process. The vanishing points of the parallel lines of the landmark provide the information for computing landmark orientation. The size of the landmark is used to compute the landmark position. Lower hardware cost is also guaranteed since only one camera is required. No equipment on the landmark is needed. No information of the vehicle location or motion is required. In fact, we can compute the vehicle motion by a sequence of landmark location estimation. A case study of the helicopter landing site location for automatic helicopter landing by using the identification marking on the landing site is presented. This case study shows a useful application of the proposed approach. Acceptable experimental results have been obtained both in simulation and in testing real images. Future works may be directed to developing systems for analyzing other landmarks, such as the heliport name marking and so on, by computer vision techniques to provide more information for automatic vehicle navigation.

References

[1] Sato M. Position and attitude estimation from an image sequence of a circle. Academic Reports, Faculty of Engineering, Tokyo Institute of Polytechnics 1995;18(1):28–35.
[2] Chou HL, Tsai WH. A new approach to robot location by house corners. Pattern Recognition 1986;19(6):439–51.
[3] Atiya S, Hager GD. Real-time vision-based robot localization. IEEE Trans Robot Automat 1993;9(6):785–800.
[4] Gilg A, Schmidt G. Landmark-oriented visual navigation of a mobile robot. IEEE Trans. Ind Electron 1994;41(4):392–7.
[5] Escalera ADL, Moreno L, Salichs MA, Armingol JM. Continuous mobile robot localization by using structured light and a geometric map. Int J System Sci. 1996;27(8):771–82.
[6] Curran A, Kyriakopoulos KJ. Sensor-based self-localization for wheeled mobile robots. J Robotic Systems 1995;12(3):163–76.
[7] Lee PS, Shen YE, Wang LL. Model-based location of automated guided vehicles in the navigation sessions by 3D computer vision. J Robotic Systems 1994;11(3):181–95.
[8] Talluri R, Aggarwal JK. Mobile robot self-location using model-image feature correspondence. IEEE Trans Robotics Automat 1996;12(1):63–77.
[9] Shih SW, Hung YP, Lin WS. Accurate linear technique for camera calibration considering lens distortion by solving an eigenvalue problem. Optical Engineering Jan. 1993;32(1):138–49.
[10] Kuo S, Cross GR. A string-matching procedure. Pattern Recognition 1991;24(7):711–6.
[11] Minnemen MJ. Handwritten character recognition employing topology, cross correlation, and decision theory. IEEE Trans Syst Sci Cybernet Dec 1996;2:86–96.
[12] International Civil Aviation Organization. Aerodromes: ANNEX 14 to the Convention on International Civil Aviation, vol. 2: Heliports. International Civil Aviation Organization, Montreal, Quebec. 1990.
[13] Wang LL, Ku PY, Tsai WH. Model-based guidance by the longest common subsequence algorithm for indoor autonomous vehicle navigation using computer vision. Automat in Construction 1993;2:123–37.
[14] Haralick RM, Shapiro LG. Computer and Robot Vision, vol. II. New York: Addison-Wesley, 1993.
[15] Noble B, Daniel JW. Applied Linear Algebra, 3rd ed. Englewood Cliffs, NJ: Prentice-Hall, 1988.
[16] Pearson DE, Robinson JA. Visual communication at very low data rates. Proc IEEE April 1985; 73(4).
[17] Gonzalez RC, Woods RE. Digital Image Processing. New York: Addison-Wesley, 1992.